Takahashi *et al.*
Progress in Earth and Planetary Science (2022) 9:66
https://doi.org/10.1186/s40645-022-00525-z

Progress in Earth and Planetary Science

RESEARCH ARTICLE

Open Access

Tectonic tremors immediately after the 2011 Tohoku-Oki earthquake detected by near-trench seafloor seismic observations

Hidenobu Takahashi[1,2*], Ryota Hino[1], Naoki Uchida[1,3], Takanori Matsuzawa[4], Yusaku Ohta[1], Syuichi Suzuki[1] and Masanao Shinohara[3]

Abstract

Temporal seismic observations from pop-up type ocean-bottom seismometers were used to detect tectonic tremors immediately following the 2011 Tohoku-Oki earthquake in the northern periphery of the aftershock area. Near-field observations clearly distinguished tremors from regular earthquakes based on their spectral shape in the frequency band of 1–4 Hz. In addition to tremors accompanied by very low-frequency earthquakes (VLFEs), we detected 130 tremors without known VLFE activity during April–October 2011. The newly detected tremors were in the vicinity of a sequence of small repeating earthquakes, indicating a mixed distribution of tremors and regular interplate earthquakes in the region. Tremor activity was high immediately after the deployment of seismometers and gradually decreased. In addition, the tremor activity fluctuated with two activations with an interval of approximately 90 days, similar to the intervals between tremor bursts after 2016. The results of the study suggest that the observed tremors occurred under the influence of aseismic slip caused by the decaying afterslip of the preceding Tohoku-Oki and Mw 7.4 interplate earthquakes and episodic accelerations with a quasi-periodicity unique to the area.

Keywords: Tectonic tremor, Ocean bottom seismometer, The 2011 off the Pacific coast of Tohoku earthquake, Slow earthquake, Aseismic slip

1 Introduction

Various types of slow earthquakes have been observed globally; their activity on subduction interfaces is expected to have a strong relationship with the generation processes of massive interplate earthquakes (e.g., Obara and Kato 2016; Kano et al. 2018). Tectonic tremors (hereafter, tremors) are a kind of slow earthquake phenomena characterized by unclear P- and S-wave arrivals with a dominant frequency of 2–8 Hz and smaller amplitudes than those of regular earthquakes with similar seismic moments. Tremors are usually active at the margins of seismogenic zones, both at the downdip (e.g., Obara 2002; Frank et al. 2014) and updip (e.g., Obana and Kodaira 2009; Todd et al. 2018) sides. The spatio-temporal correlation of tremors and other types of slow earthquakes are often observed. Spatiotemporal coincidence of tremors and very low-frequency earthquakes (VLFEs) in the seismic frequency band below 0.1 Hz has been observed in the Hyuga-nada region (Yamashita et al. 2015) and the Nankai subduction zone (Ito et al. 2007; Kaneko et al. 2018). Such a relationship between different types of slow earthquake phenomena suggests that this series of different dominant frequencies is a united broadband phenomenon (Ide 2008).

Slow earthquake activities recently became clearer along the Japan Trench subduction zone, where the 2011 Tohoku-Oki earthquake (Mw 9.1) had occurred. Via the deployment of the new cabled seafloor observation network for earthquakes and tsunamis along the

*Correspondence: takahashi3894@criepi.denken.or.jp

[1] Graduate School of Science, Tohoku University, 6-6 Aza-Aoba, Aramaki, Aoba-Ku, Sendai 980-8578, Japan
Full list of author information is available at the end of the article

Japan Trench (S-net) in 2016, Tanaka et al. (2019) and Nishikawa et al. (2019) found new tremor activity below the network. The reported tremors occurred approximately 20 km landward from the trench axis, at a depth to the plate boundary of approximately 10 km below the seafloor, representing a quasi-periodic recurrence of short-term burst activities. Based on onshore broadband seismic records, Matsuzawa et al. (2015) and Baba et al. (2020) reported VLFE activities during the period before S-net deployment until 2018. Both studies showed that the activity of the VLFEs was significant after the 2011 Tohoku-Oki earthquake in the region surrounding the rupture of the earthquake. Considering the synchronicity of tremors and VLFEs in other subduction zones (e.g., the Nankai subduction zone and the Hyuga-nada region), tremor activity is expected to increase in areas of increased VLFE activity following the Tohoku-Oki earthquake.

Recent studies have shown that the temporal deployment of ocean bottom seismometers (OBSs) in the area of possible tremor activity can aid in efficiently identifying shallow tremor activity owing to their vicinity to the tremor sources (Ito et al. 2015; Katakami et al. 2018; Todd et al. 2018). In this study, we analyze seismograms obtained from OBSs deployed in the northern Japan Trench to investigate tremor activity for approximately half a year following the Tohoku-Oki earthquake and discuss the relationship between tremors and the Tohoku-Oki earthquake.

2 Observations

To monitor the aftershock activity, five free-fall and pop-up OBSs were deployed at the northern rim of the aftershock area of the 2011 Tohoku-Oki earthquake, and observations were made from April 11 to October 25, 2011 (Fig. 1). Three-component velocity seismograms from geophones with a natural frequency of 4.5 Hz were recorded at 100 Hz sampling. The short-period OBSs cannot record the long-period signals of the VLFEs. However, if tremors and VLFEs have a common source like that observed in Nankai (Kaneko et al. 2018) and are different manifestations of a broadband phenomenon (slow earthquake), we can observe seismic signals in the tremor frequency band using short-period OBSs. During the OBS observation, seven VLFEs were identified near the OBS array based on land broad-band station data (Matsuzawa et al. 2015), which were referred to as VLFE #1–7 in the order of their occurrence. In this study, we first searched for tremors that occurred near the VLFEs in time and space.

The OBS seismograms around the origin times of the VLFEs showed a gradual increase in horizontal amplitudes with unclear P- and S-wave arrivals (Figs. 2b and 3). To investigate the hypocenter of the observed events, we focused on the amplitudes and arrival time differences among the stations since according to the hypocentral distances, the amplitudes will decrease, and the arrival time will be delayed. We observed a decrease in the amplitude in the order of the distances from the respective VLFE epicenters. We also observed the timing of peak amplitudes delayed with the increasing epicentral distances from the VLFEs. These observations suggest that the seismic signals recorded by the OBSs radiated from points near the VLFEs' epicenters.

Furthermore, the order of the timing of the peak amplitude and the spatial decay of the amplitudes observed for the events associated with the VLFEs resemble those of local repeating earthquakes and regular interplate earthquakes with epicenters located close to the VLFE epicenters. Figures 2c and 3 represent the seismograms of two repeating earthquakes: A (M3.9) and B (M2.7), respectively. We selected these two as examples considering the uncertainties of epicenters of VLFEs and earthquakes estimated by onshore seismic networks. Although seismograms of repeating earthquakes showed much larger amplitudes and clearer P- and S-wave onsets than the seismograms at the VLFE timings, the orders of arrival times and peak amplitudes at different OBSs were similar (Figs. 2d and 3). The amplitude variations among the OBSs were also similar for all seismograms at the time of the other VLFEs (Figs. 3 and 4). This characteristic indicates that the recorded events with vague onsets that dominate the horizontal component are seismic signals radiated from sources near the VLFEs.

Although the source locations of the seven events were considered near the hypocenter of repeating earthquakes, the frequency contents of the seismograms of the events were significantly different from those of repeating earthquakes. Figure 2a shows the power spectral density of the horizontal seismograms around the occurrence time of VLFE #5 and repeating earthquake-A at station AO.S05, which is nearest to VLFE #5. The power spectral density of this event had a decay pattern different from that of repeating earthquake-A in the frequency range of 1–4 Hz. The most prominent difference between the repeating earthquakes and the events identified at the VLFE occurrences is the slope of the spectra in the frequency range between 1 and 4 Hz. The slopes are significantly steeper for the repeating earthquakes. All the events synchronous with the VLFEs had a similar power spectral density shape, with the gentle slope in 1–4 Hz band (Fig. 5). As higher-frequency signals are more attenuated during propagation, deficiencies in the high-frequency component can also be identified in the seismograms of remote regular earthquakes. For example, the power spectral density below 6 Hz of the seismogram

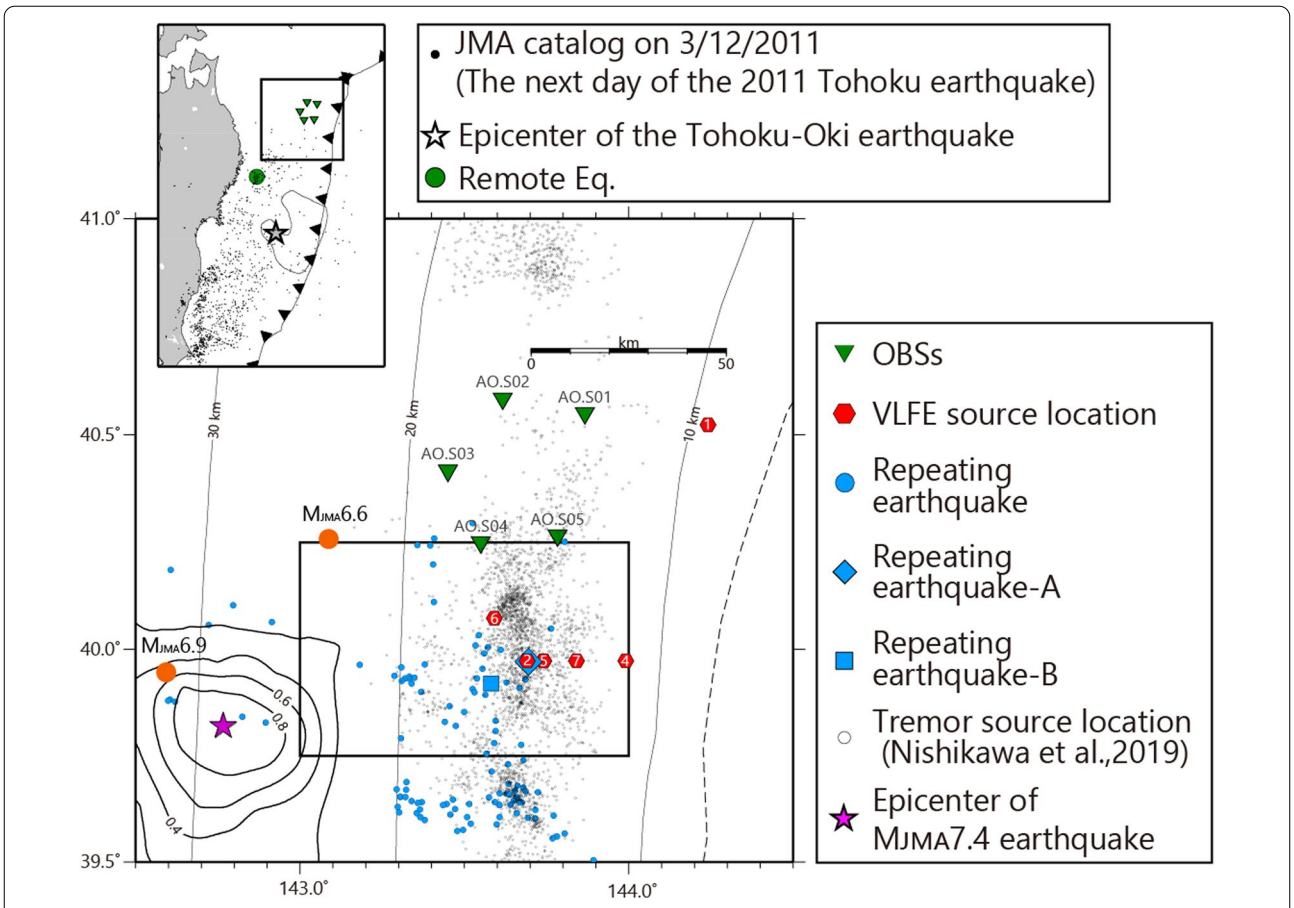

Fig. 1 Locations of ocean-bottom seismometers (OBSs) and known very low-frequency earthquakes (VLFEs). The epicenter of VLFE #3 is the same as VLFE #5. Reverse triangles and hexagons represent OBSs and VLFEs, respectively. Blue circles represent repeating earthquakes that occurred between April 10 and October 25, 2011. Diamond represents a repeating earthquake-A (M3.9) whose seismograms are compared to those of the tremors. Square represents a repeating earthquake-B (M2.7) with the closest hypocenter to tremors. The depth contours of the plate boundary (Nakajima and Hasegawa 2006) are shown by black lines. Black circles indicate the epicenters of tremors (Nishikawa et al. 2019), while dashed line indicates the trench axis of the Japan Trench. The black dots in the inset map on the upper left are Japan Meteorological Agency epicenters of regular earthquakes on March 12, 2011, defining the aftershock area of the 2011 Tohoku-Oki earthquake, whose epicenter is shown by a star

of an earthquake with an epicentral distance of approximately 160 km resembles the power spectral densities of the events identified at the VLFE timings (Figs. 2d and Additional file 1: S1). However, the spatial variation of the observed amplitudes was clearly different from that of the events associated with the VLFEs (Figs. 4). Thus, local low-frequency events can be distinguished from remote earthquakes.

Based on these observations, the similarity in amplitude variation with local repeating earthquakes, and the evident deficit of high-frequency energy, it is suggested that the events detected at the timing of the known VLFEs are seismic waves that radiated from tremors whose sources are close to those of the VLFEs and repeating earthquakes. Owing to the limitation of the observable frequency range of short-period OBSs used in this study, it is difficult to discuss the relationship between newly identified tremors and the corresponding VLFEs where tremor-VLFE pairs are regarded as single events. Hereafter, the newly identified tremor events will be referred to as tremors #1–#7, according to the number of corresponding VLFEs.

We search for the characteristic patterns of seismograms of the identified tremors associated with previously identified VLFEs in the continuous seismograms for approximately six months, so that we can identify tremors in addition to those with the VLFEs.

3 Methods

The previous section showed that short-period OBSs deployed near known VLFEs epicenters recorded tremors associated with each VLFE. Conversely, this section

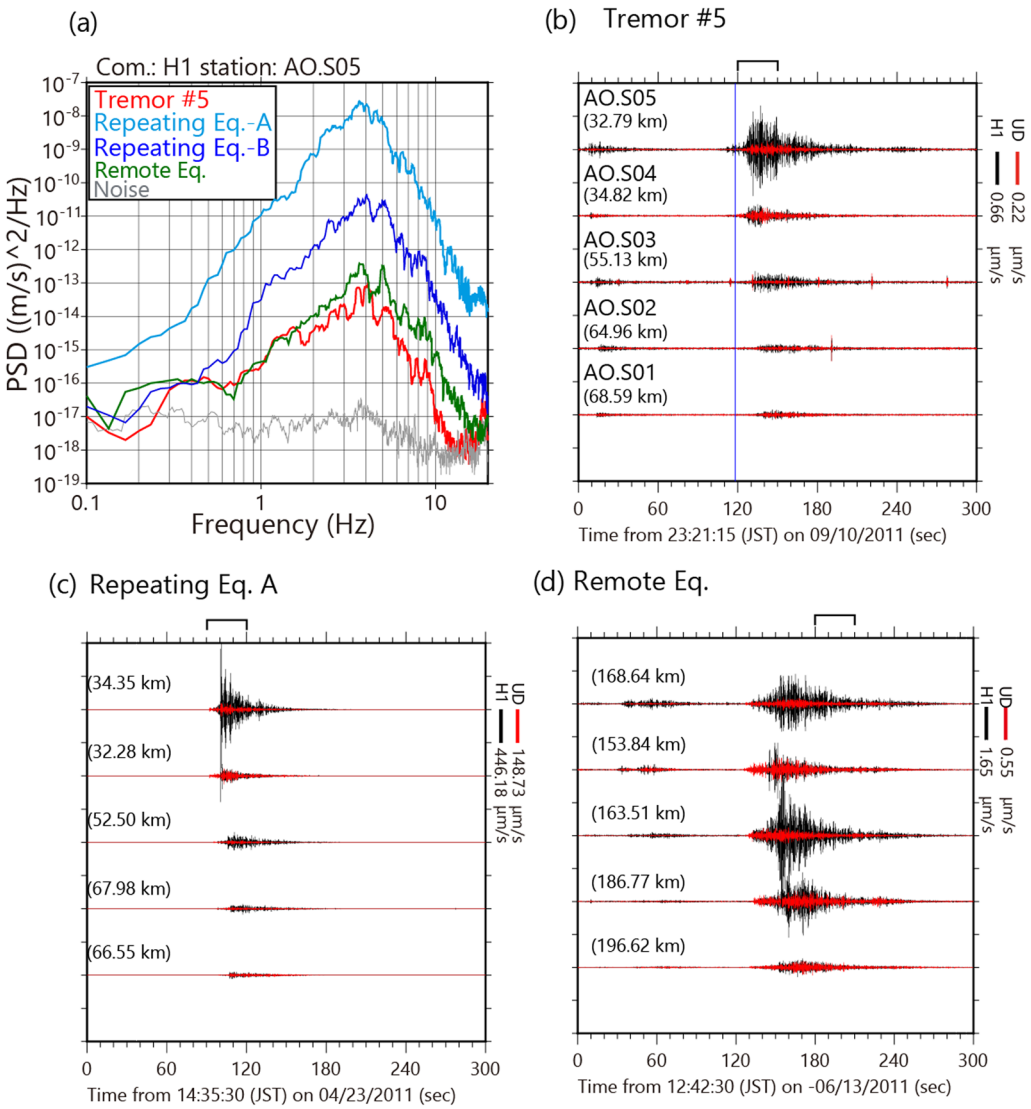

Fig. 2 Characteristics of tremors observed by the ocean-bottom seismometers (OBSs) **a** Power spectra of the tremor, the repeating earthquakes, and the remote earthquake shown in Fig. 1. Horizontal records at AO.S05 in the time window indicated by brackets in **b** are used. Background noise is taken from a window of 30 min before the origin time of known very low-frequency earthquake (VLFE) #5. (b) Filtered (2–4 Hz) seismograms during tremor #5, whose location is shown as a green circle in the left top inset of Fig. 1. Vertical and horizontal records are shown by red and black traces, respectively. Epicentral distances are shown in parentheses. The vertical blue line shows the origin time of the VLFE #5. **c** Filtered (2–4 Hz) seismograms during repeating earthquake-A, **d** Filtered (2–4 Hz) seismograms during a remote earthquake (M3.4)

investigates the tremors that are not associated with the reported VLFEs since tremors are detected more frequently than VLFEs (Ghosh et al. 2015; Ohta et al. 2019; Nishikawa et al. 2019). Generally, the envelope correlation method (Obara 2002) is effective in detecting tremors. However, the method did not work well for detecting and locating tremors, including those identified by visual inspection of the seismograms around VLFE timing. This might be because most of the tremor sources were located outside the OBS network used in the study, which consisted of only five stations, making tremor detection very difficult.

Instead, the amplitude patterns (Fig. 4) and power spectral densities (Fig. 5) can be used for identifying additional tremors because these characteristics should be similar among tremors #1–7 and new tremors that are not associated with the reported VLFEs.

We quantified the following two characteristics: First, the deviation of the peak amplitude pattern (hereafter *amplitude deviation*) from the averaged peak amplitude

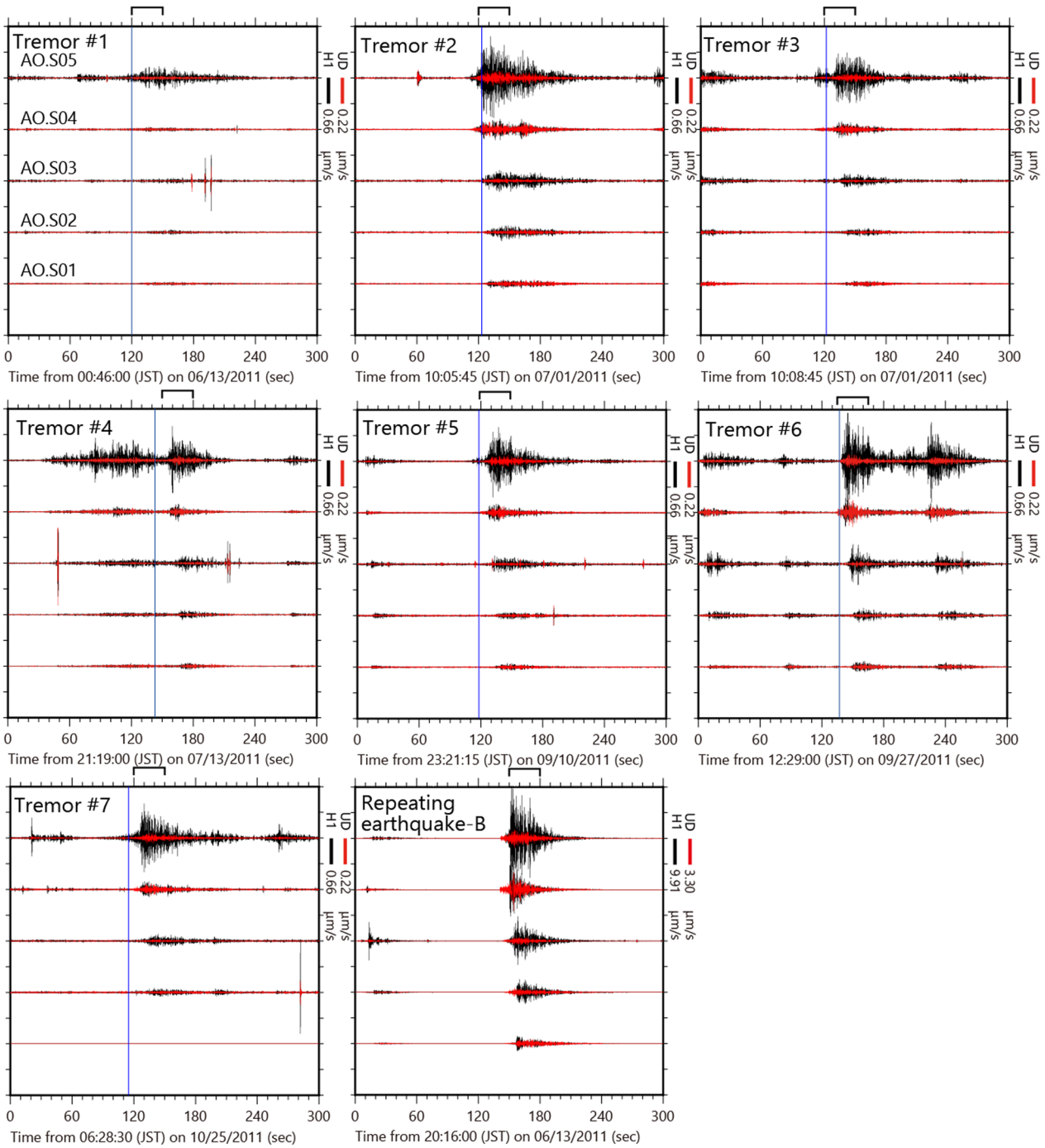

Fig. 3 Waveforms of tremor #1–7 and repeating earthquake-B. Filtered (2–4 Hz) horizontal and vertical seismograms with detected time-windows. The vertical blue line shows the origin time of the VLFE (Matsuzawa et al. 2015)

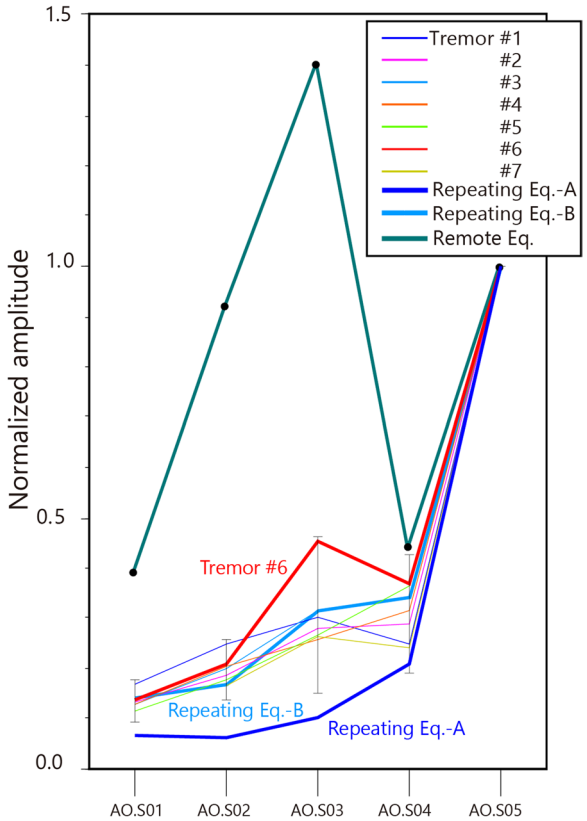

Fig. 4 Variation of maximum horizontal amplitude among the ocean-bottom seismometers (OBSs) stations. The maximum horizontal amplitudes in 2–4 Hz at four stations (AO.S01 to S04) are normalized to that at station AO.S05. Mean and standard deviations for the seven tremors are indicated by error bars

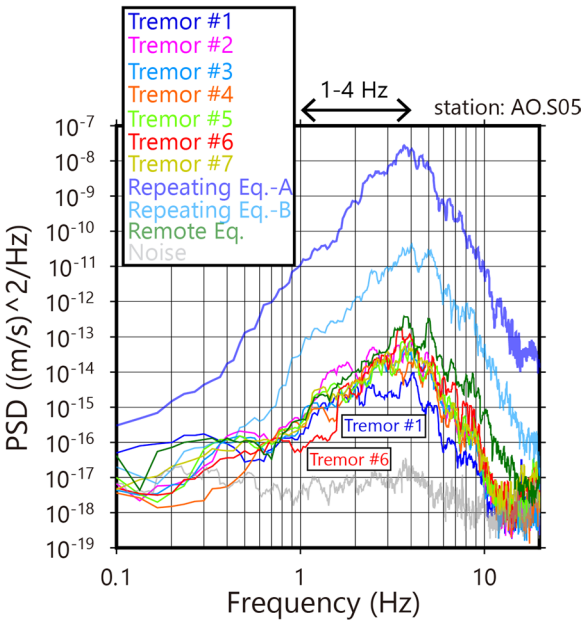

Fig. 5 Power spectral density of tremor #1–7, repeating earthquake-A and -B, remote earthquake, and background noise in horizontal components. Known very low-frequency earthquake (VLFE) #1 has lower power than those of the other tremors in all frequency bands. VLFE #6 lacks power in a frequency range of 1–2 Hz

pattern of tremors #1–7. The *amplitude deviation* was defined by the difference between the peak amplitude distribution of samples and the average distribution for the seven tremors, and is calculated as follows:

$$\text{Amplitude deviation} = \max\left(\text{AMF}_i\right)$$

and

$$\text{AMF}_i = \left|\hat{A}_i^{\text{sample}} - \overline{\hat{A}_i^{\text{ref}}}\right| / 2\sigma_i$$

$\hat{A}_i^{\text{sample}}$ is the peak horizontal amplitude at station *i*, normalized to the peak amplitude at station AO.S05. The peak values of the root-mean-squared horizontal amplitude of the sample waveforms of the records of the two horizontal components were used. $\overline{\hat{A}_i^{\text{ref}}}$ is the average of the peak amplitudes of the reference seismograms at station *i*, including tremors #1–7. The deviation from the reference at station *i* was scaled by σ_i, the standard deviation of the peak amplitudes of the seven tremors at the corresponding station *i*. The *amplitude deviation* decreased with the increase in the similarities, in terms of peak amplitude distribution, between the sample and the reference. After applying a band-pass (2–4 Hz) filter, a frequency band in which the tremor signal was most pronounced, sample seismograms were obtained from continuous seismograms using a sliding time window of 30 s with a time interval of 15 s.

Second, the residual sum of squares between the power spectral density of a sample waveform and that of tremor #5, which was observed with the highest signal-to-noise ratio (S/N), was calculated as a measure of similarity between power spectral densities. The residual sum termed *"spectral deviation"* is calculated as follows:

$$\text{Spectral deviation} = \sum_{j=1}^{N} \left(\log_{10}\text{PSD}_j^{\text{sample}} - \log_{10}\text{PSD}_j^{\text{ref}}\right)^2$$

where $\text{PSD}_j^{\text{sample}}$ represents the power spectral density of a sample seismogram and $\text{PSD}_j^{\text{ref}}$ is the power spectral density of the reference seismogram at a frequency band *j*. $N = 90$ is the number of power spectral densities within a frequency range of 1–4 Hz, where high S/N is expected. We used the records at station AO.S05 for tremor #5 for the reference seismogram, since the seismogram had the highest S/N. A higher similarity yielded a smaller *spectral*

deviation. The sample power spectral densities were calculated from the seismograms extracted using sliding time windows identical to the *amplitude deviation* calculation. *Spectral deviation* was calculated in the frequency band of 1–4 Hz. Husker et al. (2019) developed a tremor detection method based on the single-station tremor spectrum template. Our *spectral deviation* is essentially the same as that used in Husker et al. (2019), but different cost functions. Both *amplitude deviation* and *spectral deviation* take smaller values when a sampled seismogram resembles that of the tremors. We determined the length of the sliding window as 30 s after a test using different lengths (Additional file 1: Fig. S2).

A 15 s window is too short to characterize the given event in terms of maximum amplitude due to the short-term irregular fluctuation of seismograms. By contrast, a 60 s window is too long to discriminate successive occurrences of tremors.

Figure 6 shows the two-hour spectrograms with temporal variations of *amplitude* and *spectral deviations* for the period in which tremor #5 occurred. Both *amplitude* and *spectral deviations* had the smallest values at the time of tremor #5. As expected, the *amplitude* and *spectral deviations* for the seismograms obtained in the seven windows including the occurrence times of tremors #1–7 were considerably smaller than the rest of the seismograms in the six days when the seven tremors with the VLFEs were detected (Fig. 7).

Notably, *spectral deviation* of tremor #1 was relatively large due to low signal levels (Figs. 3 and 5). Tremor #6, which was depleted in the low (1 Hz) frequency components more than other tremors (Fig. 5) and slightly deviated from other tremors in terms of peak amplitude distribution (Fig. 4), had a larger *amplitude* and *spectral deviations*. For more conservative tremor detection, these two events (tremors #1 and #6) were excluded while defining the thresholds of *amplitude* and *spectral deviations*. Therefore, based on the *amplitude* and *spectral deviations* for tremors #2–5 and #7, the thresholds were set at 0.675 and 0.17 for *amplitude* and *spectral deviations*, respectively (Fig. 7).

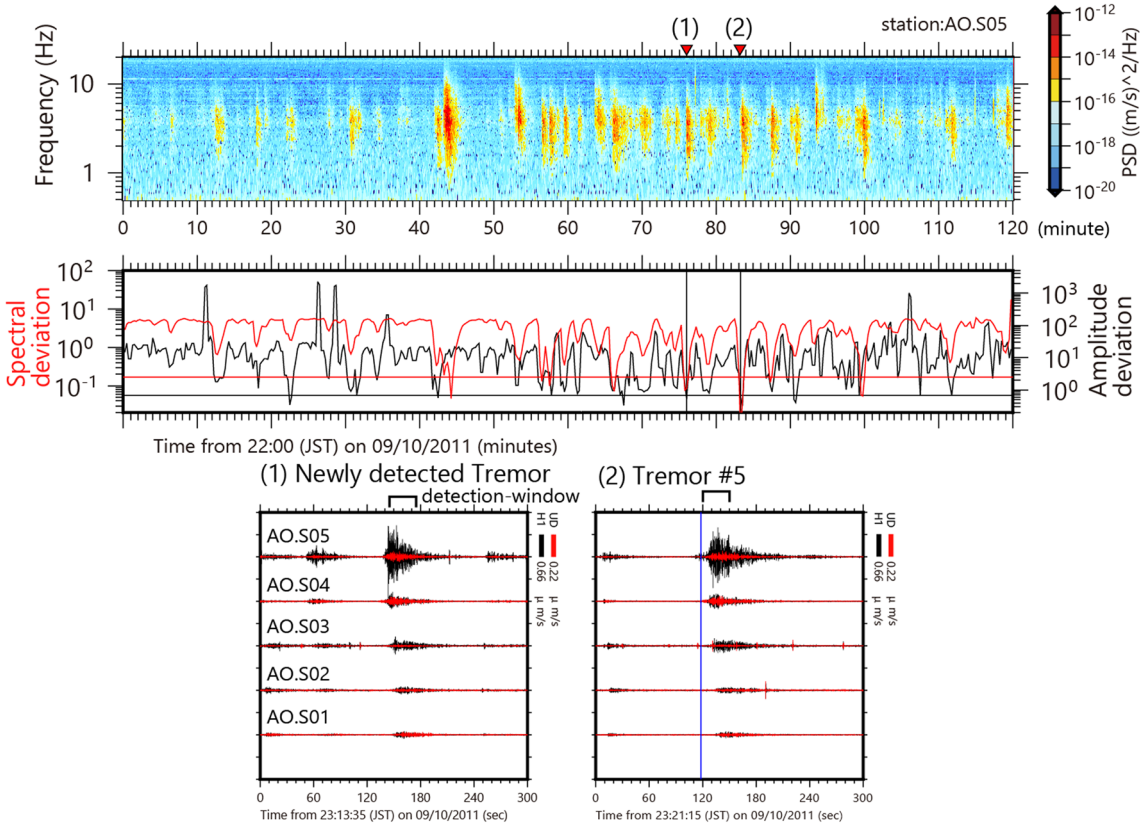

Fig. 6 Two-hour spectrogram of the horizontal component at AO.S05 (top), with temporal variation of *amplitude* and *spectral deviations* (middle), and seismograms of two identified tremors, (1) and (2), (bottom). Horizontal red and black lines in the middle panel show the detection threshold of *spectral* and *amplitude deviations*, respectively. Vertical and horizontal component records are indicated by red and black traces, respectively, in the bottom panel

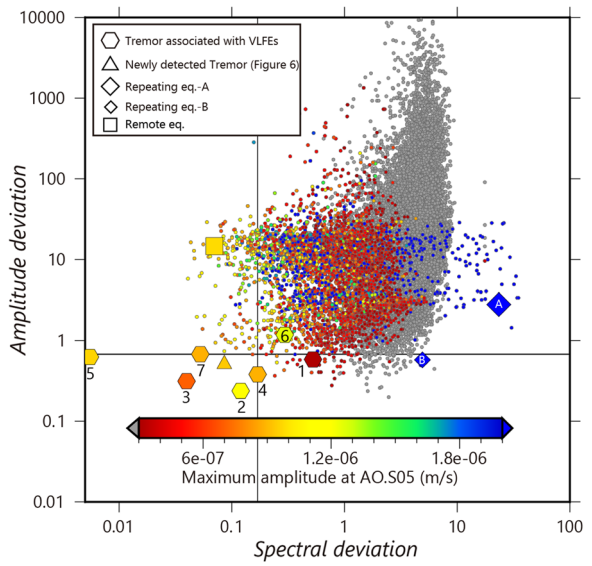

Fig. 7 Results of waveform classification using *amplitude deviation* and *spectral deviation* for the six days when the reported very low frequency earthquakes (VLFEs) occurred. Hexagons represent tremors #1–7, diamonds represent repeating earthquakes, and a square represents remote earthquake. Symbol colors show the maximum amplitude at station AO.S05 at the corresponding time window. Thresholds of *spectral* and *amplitude deviations* are shown by vertical and horizontal lines, respectively. The *spectral* and *amplitude deviations* calculated for repeating earthquake-A, repeating earthquake-B, and a remote earthquake are also shown, although these earthquakes occurred on different days. The *spectral deviation* of tremor #5 is not exactly zero in the figure since the time window including tremor #5 in the event search is slightly different from that for the reference power spectral density calculation

Based on the proximity of the epicenters of repeating earthquakes to those of the VLFEs, the *amplitude deviations* of repeating earthquakes are expected to be as small as those of tremors. The *amplitude deviation* of repeating earthquake-A was not smaller than the criteria (Fig. 7), whereas that of repeating earthquake-B was smaller than the threshold for tremor detection. This suggests that repeating earthquake-B, a regular earthquake, occurred very close to the sources of the tremors. By contrast, *spectral deviations* of repeating earthquakes are different from those of tremors.

In the seismogram of the remote earthquake shown in Fig. 1, *spectral deviation* is smaller, but *amplitude deviation* is larger than the thresholds (Fig. 7). However, *spectral deviation* of the remote earthquake is similar to those of tremors.

Therefore, tremors can be distinguished from local and remote regular earthquakes by *amplitude* and *spectral deviations*. As shown by the triangle in Fig. 7, a seismogram satisfied the criteria of tremor detection during the six days. Figure 6 shows the corresponding record as an event 10 min before tremor #5. The newly detected event was similar to tremor #5 in the seismograms, and it can be regarded as another tremor event. There were a few events that satisfied the tremor detection threshold of *spectral deviation* but not that of *amplitude deviation* (*e.g.*, events at 87 min and 100 min in Fig. 6). The slightly larger *amplitude deviation* but acceptably small *spectral deviation* of these events indicate that these events can be tremors with different source locations from the group of tremors identified in the study.

4 Results

We identified a total of 131 tremors other than the events associated with the known VLFEs by inspecting ~ 6 months continuous OBS waveforms based on the two parameters *amplitude* and *spectral deviations* (Additional file 1: Fig. S3). The *amplitude* and *spectral deviations* (Additional file 1: Fig. S3), and waveform characteristics (Fig. 8) of the newly identified tremors were similar to those of the known tremors associated with known VLFEs described in Sect. 2. For most of the events, the windows satisfying the criteria were isolated, although sometimes two successive windows satisfied the thresholds. However, both *amplitude* and *spectral deviations* were not sufficiently low in three or more successive windows. This suggests that the duration of tremors detected here was not significantly longer than 60 s, i.e., twice the window length. This result is consistent with the reported average duration of tremors (44 s) in the northern Japan Trench (Nishikawa et al. 2019).

As defined above, *spectral deviation* is the difference of the absolute power spectral densities to that of tremor #5; the detected events should have a similar size to that of tremor #5. If the present threshold based on the *spectral deviation* was used, tremor events of different magnitudes would be missed.

Smaller events are difficult to identify using *amplitude deviation* as the reliability of event identification using *amplitude deviation* is dependent on the S/N ratio of seismograms, and small tremor events with a smaller S/N ratio, if they existed, would be rejected. Therefore, to identify possible large-tremor events, the power spectral densities of all events with an S/N ratio larger than that of event #5 were analyzed. The magnitudes of the events were measured by calculating the average of the power in the 1–4 Hz frequency range. As indicated in Sect. 2, there is an evident difference in the slopes of power spectra in this frequency range between regular earthquakes and tremors, hence we attempted to determine whether the large events are classified as tremors or regular earthquakes.

The magnitude of only a few events, among the events with acceptably small *amplitude deviation*, were larger than that of tremor #5, which was used as a reference for tremor search (Fig. 9). Most of the events, including repeating earthquake-B, had steeper power spectral density slopes than tremor #5, indicating regular earthquakes rich in

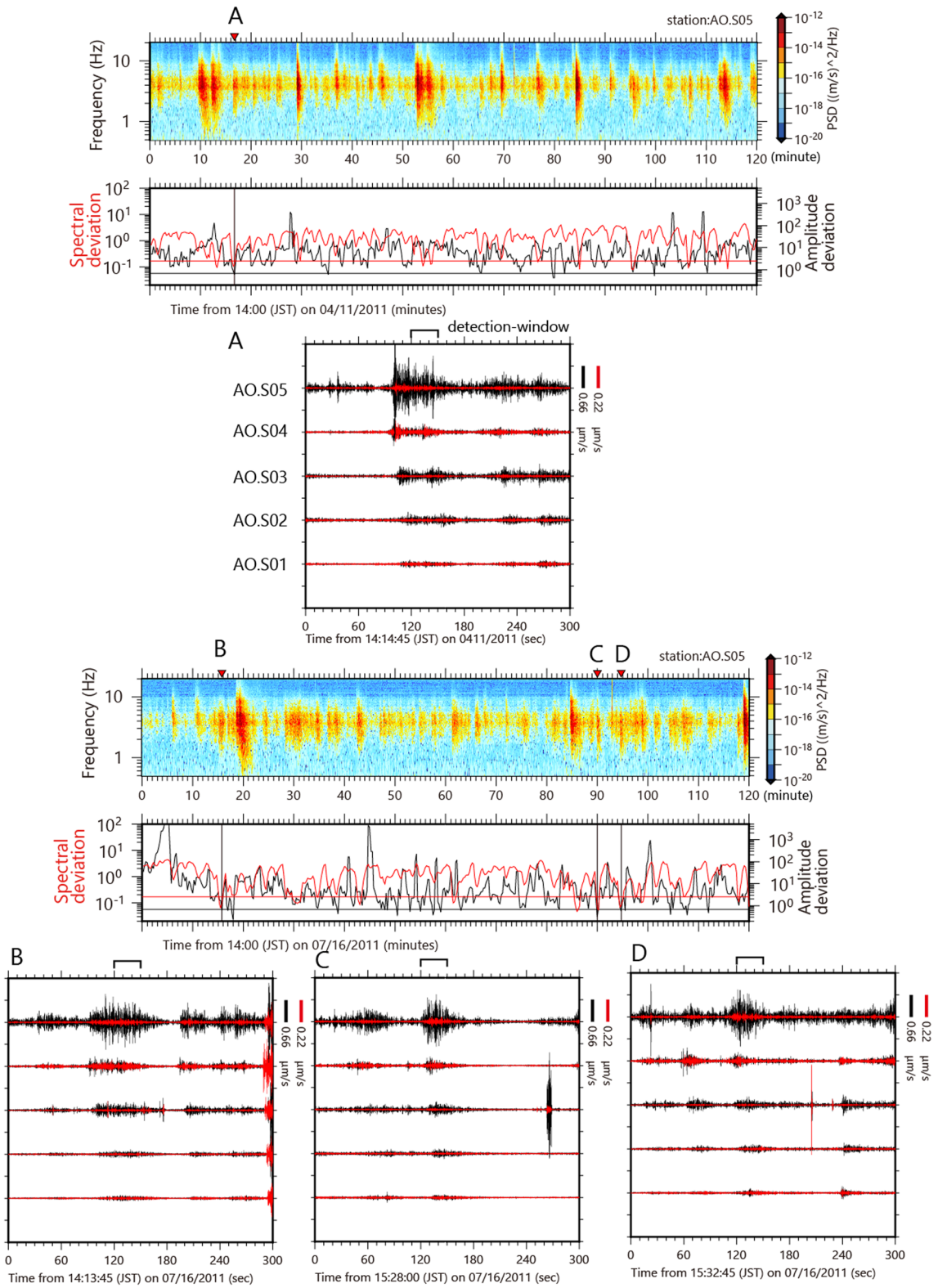

Fig. 8 Examples of newly detected tremors. Two-hour spectrograms of horizontal components, including a tremor (upper) and three tremors (lower) are shown with temporal variations in *amplitude* and *spectral deviations*. Red inverted triangles at the top of the spectrograms represent the detection times of the tremors and seismograms of corresponding tremors

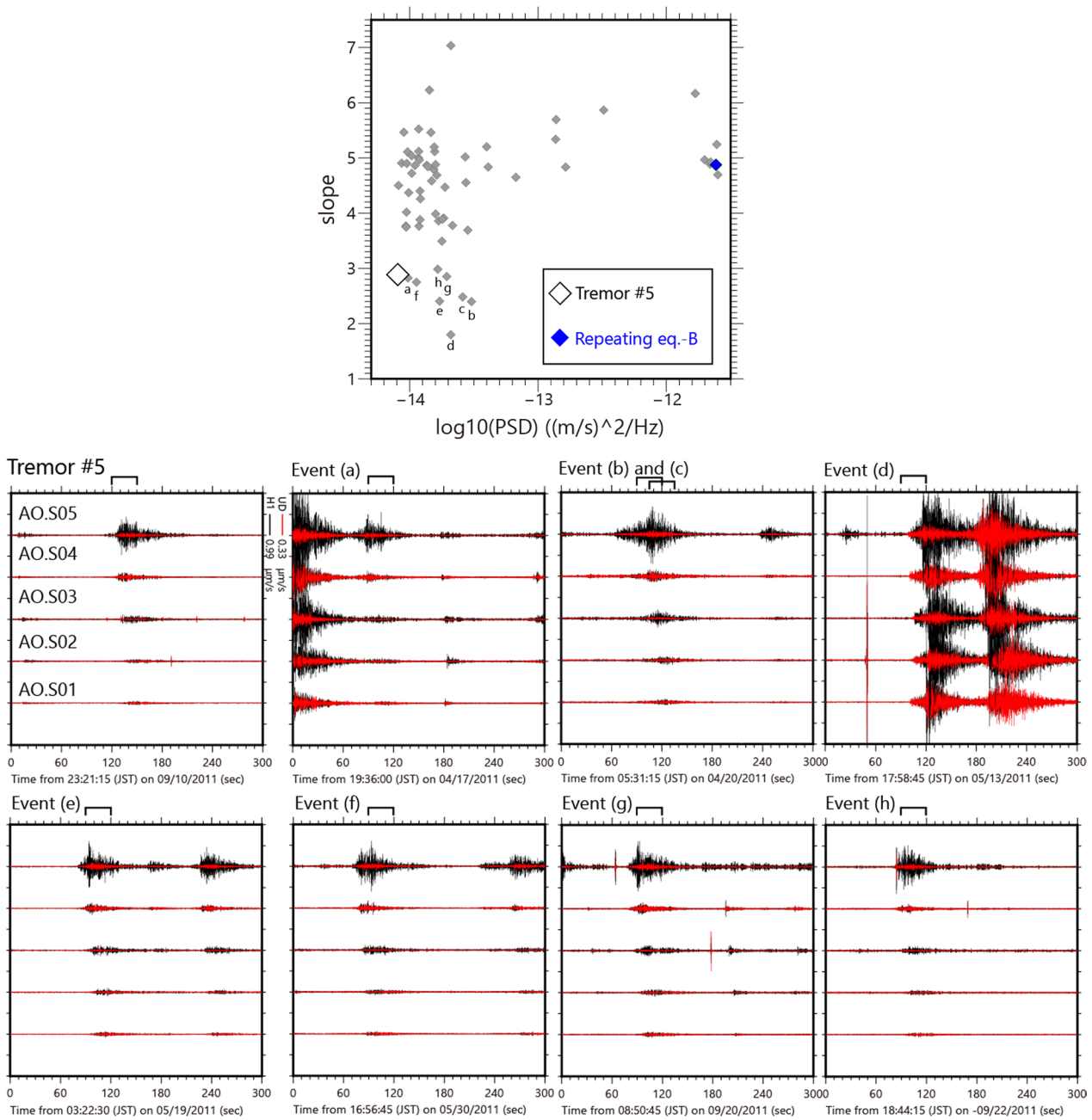

Fig. 9 Relationship between slope of power spectral density at 1–4 Hz, and average of power at 2–4 Hz band for the events with *amplitude deviation* smaller than the tremor detection threshold. The waveforms of the events showing power spectral density slopes similar to or smaller than that of tremor #5 (indicated as a to h in the top panel) are shown in the bottom two rows. The red and black lines show vertical and horizontal components, respectively. The brackets show the locations of the detection windows

high-frequency content. Nevertheless, we detected a small number of large events having a small power spectral density slope that were relatively rich in low-frequency content. Except for a single event (d in Fig. 9) that corresponds to the P-coda part of a remote regular earthquake (M3.8), the waveforms of these events resemble those of tremor #5. These low-frequency events may be slightly larger than tremor #5. These observations suggest that only the largest tremors in the study area were detected in this study.

5 Discussion

Since the tremor detection method relies on the similarities of the spatial pattern of the peak amplitudes at different stations, the sources of all detected tremors,

including those accompanied by the seven VLFEs that are used as references, were concentrated within a small area. Notably, the signal amplitude distribution of repeating earthquake-B was very similar to that of the tremors (Fig. 3), ensuring that the *amplitude deviation* of repeating earthquake-B was as small as the *amplitude deviation* of tremors (Fig. 7). The similarity of the amplitude variations requires the proximity of the hypocenters and the focal mechanisms, hence the observations in this study suggest that the detected tremors were thrust faulting events in the vicinity of repeating earthquake-B, a regular interplate earthquake. The repeating earthquakes were relocated using P-wave arrivals at five OBS stations to confirm the correlation between their epicentral locations and *amplitude deviation*. As a result, the closest earthquake to the repeating earthquake-B was ~ 3 km away and had larger *amplitude deviation* than the tremor detection threshold (Fig. 10), with one exception (repeating earthquake-B'), which belongs to the sequence of repeating earthquake-B and was considered a re-rupture of the identical source area for repeating earthquake-B. Based on the relocated epicenters, repeating earthquakes with *amplitude deviation* larger than the tremor detection threshold were more than 5 km away from repeating earthquake-B. This suggests that *amplitude deviation* can be used to distinguish epicentral locations at a resolution of approximately 5 km and that newly detected tremors occurred within 5 km of regular interplate earthquakes (repeating earthquake-B and -B'). These results confirm the close association of tremors and regular earthquakes along the Japan Trench Subduction Zone. By contrast, such mixed distributions of tremors and regular earthquakes are rarely observed in the Nankai subduction zone (Obara and Kato 2016; Takagi et al. 2019; Uchida et al. 2020).

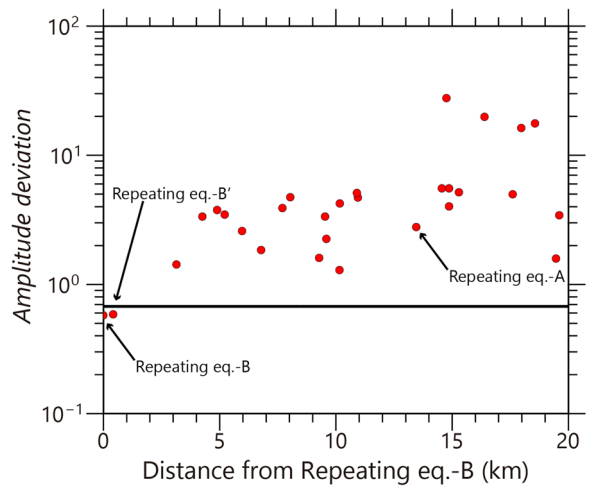

Fig. 10 Dependence of *amplitude deviation* on the inter-event distances of repeating earthquakes located around the tremor #5 measured from repeating earthquake-B by the Japan Meteorological Agency. Distances are calculated based on the relocated hypocenters by the present study using manual P-readings of five ocean-bottom seismometers (OBSs). Only repeating earthquakes within 20 km are shown. A horizontal line shows the threshold of *AI* for tremor detection

Tremors occurred continuously throughout the observation period, with notable temporal variations in the number of tremors (Fig. 11(a)). The tremor activity area covered in this study is located on the updip side of the rupture zone of the Mw 7.4 earthquake that occurred at 15:08 on 2011/03/11 (JST) (Fig. 1a), 22 min after the Mw 9.1 Tohoku-Oki earthquake. Kubo and Nishikawa (2020) suggested that slow earthquakes are generally active in this area. The results of this study recorded the tremors associated with such slow earthquakes. As pointed out by Kubo and Nishikawa (2020), this is also the area where aftershocks of the Mw 7.4 earthquake were concentrated. The temporal variation in the number of tremors detected in this study was very similar to that in the number of earthquakes that occurred around the tremor location (Fig. 11c). The similarity between the number of aftershocks and the time variation of postseismic deformation often suggests that aftershocks are triggered by afterslips (Perfettini and Avouac 2004). Since tremors are primarily caused by aseismic slip, the similarity in the temporal variation of the aftershock activity and the number of detected tremors suggests that they were both induced by a common aseismic slip, namely the afterslip of the Tohoku-Oki and the Mw 7.4 earthquakes.

Here, the number of repeating earthquakes and VLFEs detected immediately following the mainshock of 2011 was not large, although these events were promoted by the post-2011 aseismic slip as the tremors were. We

(See figure on next page.)

Fig. 11 The number of detected events of various types in a 15-day interval following the occurrence of the mainshocks. **a** The number of tremors in 2011 identified in the present study. Time period before ocean-bottom seismometer (OBS) deployment (April 11, 2011) is covered. The vertical dashed lines show the occurrence times of M6.9 and M6.6 earthquakes. **b** Schematic illustration of aseismic slip behavior as suggested by the tremor activity. **c** The number of all the regular earthquakes reported by the Japan Meteorological Agency in 2011. The area of the rectangle in Fig. 1 is the same as that for repeating earthquakes. **d** The number of regular earthquakes reported by Japan Meteorological Agency post the Mw 7.1 Sanriku-Oki earthquake on 2 November 1989. **e** The number of repeating earthquakes in 2011 (Uchida and Matsuzawa 2013). **f** The number of repeating earthquakes in 1989 (Uchida and Matsuzawa 2013). **g** The number of very low frequency earthquakes (VLFEs) recorded in 2011 (Baba et al. 2020). Timings of the seven VLFEs reported by Matsuzawa et al. (2015) are indicated by inverted triangles

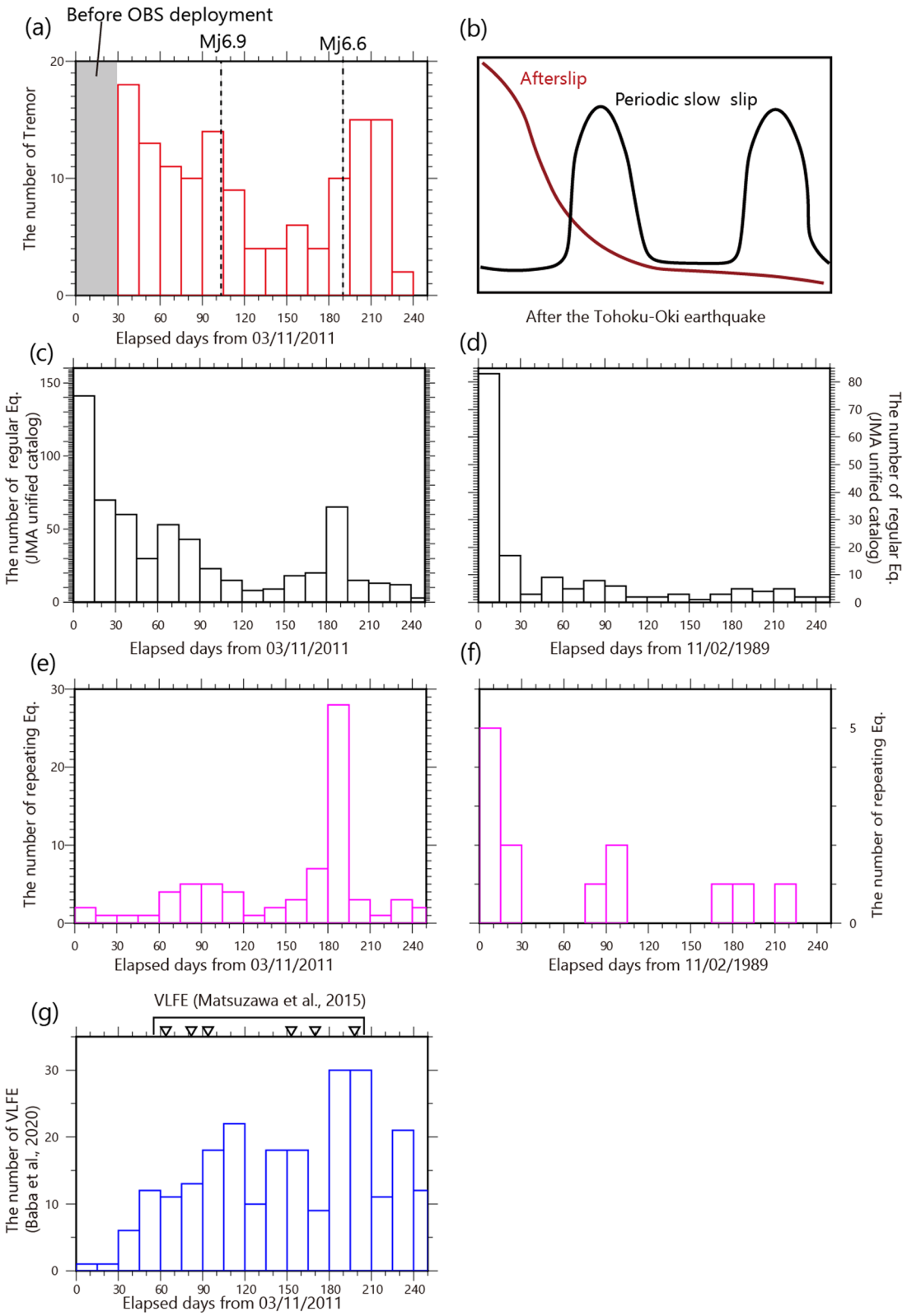

Fig. 11 (See legend on previous page.)

suspect that the extremely high seismic activity in the entire Tohoku region immediately following the M9 Tohoku-Oki earthquake may have degraded the detection abilities of the repeating earthquakes and VLFEs, thereby lowering the detected number of these events. Detection of these events requires high S/N onshore seismic waveform records. The unusually high seismic activity might have also reduced VLFEs detection. After the 1989 earthquake, which had similar coseismic slip area and aftershock distributions to those of the 2011 Mw 7.4 earthquake (Kubo and Nishikawa 2020), the number of repeating earthquakes increased with the overall number of earthquakes (Fig. 11 (f)). Therefore, we argue that the repeating earthquakes, along with VLFEs, would have been much more active than the event counts.

Furthermore, from the temporal variations of the numbers of tremors and aftershocks, these activities did not show the expected monotonic time decay for the afterslips (Helmstetter and Shaw 2009), with activity maxima at approximately 90 and 180 days post the Mw 7.4 mainshock. Notably, the activities of repeating earthquake and VLFE increased synchronously around 180 days (Figs. 11e and g, respectively). The observed synchronicity of the activities of aftershocks, tremors, repeating earthquakes, and VLFEs can be interpreted as the occurrence of two transient accelerations of aseismic slip (Fig. 11 (b)). We noted that two relatively large earthquakes (Fig. 1; Mjma = 6.6 and 6.9, orange circles) had also occurred close to the study area in the middle and early period of the activity centered 90 and 180 days following the Mw 7.4 mainshock (Fig. 11a and Additional file 1: Fig. S4). However, the temporal relationship between the M ~ 6 earthquakes and tremor activities was not obvious (Additional file 1: Fig. S4). The increase in the number of tremors preceded the occurrence of Mj6.9 earthquake, whereas the Mj6.6 earthquake preceded the increase of the detected tremors, indicating that the afterslip of M ~ 6 earthquakes did not necessarily account for the activation of tremors. As Uchida et al. (2016) reported, spontaneous slow slips may trigger large earthquakes, while increase of tremor activity may be followed by an M ~ 6 earthquake.

Notably, the tremor activity after the 2016 (after the deployment of S-net) showed evident temporal fluctuations with an interval of approximately 60 to 90 days in the area, although not completely periodic (Nishikawa et al. 2019). In 2011, the time interval was close to that of episodic events in postseismic activities. In this region, small-scale slow slip events may recur quasi-periodically, not only after major earthquakes but also under interseismic steady-state conditions. Uchida et al. (2016) pointed out that periodic slow slip events occur along the Japan Trench, but the interval between the slow slip events in this region was estimated at approximately three years, which was significantly different. Thus, aseismic slip events at various timescales may coexist in this area.

6 Conclusions

Based on temporal seismic observations using pop-up-type OBSs, this study attempted to detect tectonic tremors immediately following the 2011 Tohoku-Oki earthquake in the northern periphery of the aftershock area. The tremors were distinguished from regular earthquakes based on their spectral shape in the frequency band of 1–4 Hz. In addition to the 7 tremors accompanied by VLFEs, more than 130 tremors without known VLFE activity were detected during the observation period of April–October 2011. The newly detected tremors were in the vicinity of a sequence of small repeating earthquakes, indicating a mixed distribution of tremors and regular interplate earthquakes in the region. Tremor activity was high immediately post OBS deployment and gradually decreased. In addition, the activity fluctuated with two activations with an interval of approximately 90 days, similar to the intervals between tremor bursts after the 2016 earthquake. The results suggest that the observed tremors occurred under the influence of aseismic slip caused by decaying afterslip of preceding Tohoku-Oki and Mw 7.4 interplate earthquakes and episodic accelerations with a quasi-periodicity unique to the area.

Abbreviations

OBS: Ocean-bottom seismometer; VLFE: Very low frequency earthquake.

Supplementary Information

The online version contains supplementary material available at https://doi.org/10.1186/s40645-022-00525-z.

Additional file 1. **Figure S1**. Waveforms of the remote earthqukaes and corresponding epicenters. Rectangles indicate the study area shown in Figure 1. **Figure S2.** Two-hour spectrograms with the occurrence time of VLFE #5 and corresponding Amplitude deviation and Spectral deviation with different time-windows. Red inverted triangle indicates the occurrence time of VLFE, while vertical black lines show the time with satisfaction with two thresholds. **Figure S3.** Classification results of the entire period. Red hexagons represent tremors #1–7, and open hexagons represent the other 131 tremors detected with two-dimensional frequency distribution of amplitude deviation and Spectral deviation. **Figure S4.** The number of tremors in 2011 identified in the present study. This figure resembles that of Figure 11a, except with enlarged views for the two prominent activities. (a) The number of tremors per day between 70 and 130 from 03/11/2011. (b) The numbers of tremors per day between 180 and 240 days from 03/11/2011. (c) The number of tremors during observations per 15 days from 03/11/2011. Vertical dashed lines show the occurrence times of M6.9 and M6.6 earthquakes.

Acknowledgements

We thank the captain, crew, and scientists on Kaiko Maru No. 7 and R/V Hakuho Maru (JAMSTEC) for acquiring the ocean bottom seismometer data in cruise KH11–09. We also thank the editor Prof. Roland Burgmann. Fruitful comments by reviewer Dr. William Frank and his student, Ms. Caroline Mouchon,

and an anonymous reviewer improved this manuscript. The earthquake catalog was provided by the Japan Meteorological Agency (http://www.data.jma.go.jp/svd/eqev/data/bulletin/eqdoc_e.html). We would like to thank Editage (www.editage.jp) for the English language editing. Some figures were created using generic mapping tools (Wessel et al. 2013).

Author contributions
Data analysis and manuscript preparation were performed by HT. RH, TM, and NU supervised the study at all stages. YO, MS, and SS participated in study design and discussion. All authors have read and approved the final manuscript.

Funding
This study was supported by JSPS KAKENHI (23900002, 26000002, 17KK0081, 19H05596, and 21H05206).

Availability of data and materials
The datasets used and analyzed during the current study are available from the corresponding author upon request.

Declarations

Competing interests
The authors declare that they have no competing interest.

Author details
[1]Graduate School of Science, Tohoku University, 6-6 Aza-Aoba, Aramaki, Aoba-Ku, Sendai 980-8578, Japan. [2]Present Address: Central Research Institute of Electric Power Industry, Abiko 270-1194, Japan. [3]Earthquake Research Institute, University of Tokyo, Tokyo 113-0032, Japan. [4]National Research Institute for Earth Science and Disaster Resilience, Tsukuba, Ibaraki 305-0006, Japan.

Received: 26 May 2022 Accepted: 21 November 2022
Published online: 07 December 2022

References

Baba S, Takeo A, Obara K, Matsuzawa T, Maeda T (2020) Comprehensive detection of very low frequency earthquakes off the Hokkaido and Tohoku Pacific coasts, Northeastern Japan. J Geophys Res 125:e2019JB017988. https://doi.org/10.1029/2019JB017988

Frank WB, Shapiro NM, Husker AL, Kostoglodov V, Romanenko A, Campillo M (2014) Using systematically characterized low-frequency earthquakes as a fault probe in Guerrero. Mexico, J Geophys Res 119(10):7686–7700. https://doi.org/10.1002/2014JB011457

Ghosh A, Huesca-Pérez E, Brodsky E, Ito Y (2015) Very low frequency earthquakes in Cascadia migrate with tremor. Geophys Res Lett 42(9):3228–3232. https://doi.org/10.1002/2015GL063286

Helmstetter A, Shaw BE (2009) Afterslip and aftershocks in the rate-and-state friction law. J Geophys Res. https://doi.org/10.1029/2007JB005077

Husker A, Frank WB, Gonzalez G, Avila L, Kostoglodov V, Kazachkina E (2019) Characteristic tectonic tremor activity observed over multiple slow slip cycles in the Mexican subduction zone. J Geophys Res 124(1):599–608. https://doi.org/10.1029/2018JB016517

Ide S (2008) A Brownian walk model for slow earthquakes. Geophys Res Lett 35(17):L17301. https://doi.org/10.1029/2008GL034821

Ito Y, Obara K, Shiomi K, Sekine S, Hirose H (2007) Slow earthquakes coincident with episodic tremors and slow slip events. Science 315(5811):503–506. https://doi.org/10.1126/science.1134454

Ito Y, Hino R, Suzuki S, Kaneda Y (2015) Episodic tremor and slip near the Japan Trench prior to the 2011 Tohoku-Oki earthquake. Geophys Res Lett 42(6):1725–1731. https://doi.org/10.1002/2014GL062986

Kaneko L, Ide S, Nakano M (2018) Slow earthquakes in the microseism frequency band (0.1–1.0 Hz) off Kii Peninsula, Japan. Geophys Res Lett 45(6):2618–2624. https://doi.org/10.1002/2017GL076773

Kano M, Aso N, Matsuzawa T, Ide S, Annoura S, Arai R, Baba S, Bostock M, Chao K, Heki K, Itaba S (2018) Development of a slow earthquake database. Seismol Res Lett 89(4):1566–1575. https://doi.org/10.1785/0220180021

Katakami S, Ito Y, Ohta K, Hino R, Suzuki S, Shinohara M (2018) Spatiotemporal variation of tectonic tremor activity before the Tohoku-Oki Earthquake. J Geophys Res Solid Earth 123:9676–9688. https://doi.org/10.1029/2018JB016651

Kubo H, Nishikawa T (2020) Relationship of preseismic, coseismic, and postseismic fault ruptures of two large interplate aftershocks of the 2011 Tohoku earthquake with slow-earthquake activity. Sci Rep 10(1):1–10. https://doi.org/10.1038/s41598-020-68692-x

Matsuzawa T, Asano Y, Obara K (2015) Very low frequency earthquakes off the Pacific coast of Tohoku. Japan Geophys Res Lett 42(11):4318–4325. https://doi.org/10.1002/2015GL063959

Nakajima J, Hasegawa A (2006) Anomalous low-velocity zone and linear alignment of seismicity along it in the subducted Pacific slab beneath Kanto, Japan: reactivation of subducted fracture zone? Geophys Res Lett 33(16):L16309. https://doi.org/10.1029/2006GL026773

Nishikawa T, Matsuzawa T, Ohta K, Uchida N, Nishimura T, Ide S (2019) The slow earthquake spectrum in the Japan Trench illuminated by the S–net seafloor observatories. Science 365(6455):808–813. https://doi.org/10.1126/science.aax5618

Obana K, Kodaira S (2009) Low-frequency tremors associated with reverse faults in a shallow accretionary prism. Earth Planet Sci Lett 287(1–2):168–174. https://doi.org/10.1016/j.epsl.2009.08.005

Obara K (2002) Nonvolcanic deep tremor associated with subduction in southwest Japan. Science 296(5573):1679–1681. https://doi.org/10.1126/science.1070378

Obara K, Kato A (2016) Connecting slow earthquakes to huge earthquakes. Science 353:253–257. https://doi.org/10.1126/science.aaf1512

Ohta K, Ito Y, Hino R, Ohyanagi S, Matsuzawa T, Shiobara H, Shinohara M (2019) Tremor and inferred slow slip associated with afterslip of the 2011 Tohoku earthquake. Geophys Res Lett 46(9):4591–4598. https://doi.org/10.1029/2019GL082468

Perfettini H, Avouac JP (2004) Postseismic relaxation driven by brittle creep: a possible mechanism to reconcile geodetic measurements and the decay rate of aftershocks, application to the Chi-Chi earthquake, Taiwan. J Geophys Res. https://doi.org/10.1029/2003JB002488

Takagi R, Uchida N, Obara K (2019) Along-strike variation and migration of long-term slow slip events in the western Nankai subduction zone, Japan. J Geophys Res Solid Earth 124:3853–3880. https://doi.org/10.1029/2018JB016738

Tanaka S, Matsuzawa T, Asano Y (2019) Shallow low-frequency tremor in the northern Japan Trench subduction zone. Geophys Res Lett 46(10):5217–5224. https://doi.org/10.1029/2019GL082817

Todd EK, Schwartz SY, Mochizuki K, Wallace LM, Sheehan AF, Webb SC, Williams CA, Nakai J, Yarce J, Fry B, Henrys S (2018) Earthquakes and tremor linked to seamount subduction during shallow slow slip at the Hikurangi margin, New Zealand. J Geophys Res Solid Earth 123(8):6769–6783. https://doi.org/10.1029/2018JB016136

Uchida N, Matsuzawa T (2013) Pre-and postseismic slow slip surrounding the 2011 Tohoku-oki earthquake rupture. Earth Planet Sci Lett 374:81–91. https://doi.org/10.1016/j.epsl.2013.05.021

Uchida N, Iinuma T, Nadeau RM, Bürgmann R, Hino R (2016) Periodic slow slip triggers megathrust zone earthquakes in northeastern Japan. Science 351(6272):488–492. https://doi.org/10.1126/science.aad3108

Uchida N, Takagi R, Asano Y, Obara K (2020) Migration of shallow and deep slow earthquakes toward the locked segment of the Nankai megathrust. Earth Planet Sci Lett 531:115986. https://doi.org/10.1016/j.epsl.2019.115986

Yamashita Y, Yakiwara H, Asano Y, Shimizu H, Uchida K, Hirano S, Umakoshi K, Miyamachi H, Nakamoto M, Fukui M, Kamizono M (2015) Migrating tremor off southern Kyushu as evidence for slow slip of a shallow subduction interface. Science 348(6235):676–679. https://doi.org/10.1126/science.aaa4242

Wessel P, Smith WHF, Scharroo R, Luis J, Wobbe J (2013) Generic Mapping Tools: Improved Version Released. Eos Transa Am Geophys Union 94(45):409–410. https://doi.org/10.1002/2013EO450001

Publisher's Note